



SCALAR AND VECTOR-IM-BASED DRIFT HAZARD ESTIMATIONS FOR STEEL BUILDINGS WITH ALTERNATIVE FRAMING CONFIGURATIONS

C. Málaga-Chuquitaype⁽¹⁾, K. Bougatsas⁽²⁾

⁽¹⁾ Lecturer, Department of Civil and Environmental Engineering, Imperial College London, c.malaga@imperial.ac.uk

⁽²⁾ MSc Student, Dep. Civil and Environmental Engineering, Imperial College London, konstantinos.bougatsas14@alumni.imperial.ac.uk

Abstract

Distinct structural systems prevail in different regions of the world depending on the construction skills, history and industrial context of each particular community. Japanese engineers have usually adopted a two-way layout consisting of 3D beam-column assemblages designed to resist seismic and gravity loads simultaneously. By contrast, American and European seismic codes differentiate clearly between primary and secondary lateral resisting systems and seek to provide adequate seismic strength and ductility to the primary frames while the secondary (or gravity) frames are designed to carry gravity loads only. This study examines the seismic performance of steel buildings with alternative framing systems subjected to bi-directional ground-motion. Peak drifts of one-way and two-way frames are assessed by means of scalar and vector-valued probabilistic methods. Extensive non-linear response history analyses over idealized 3D structures representing 6- and 9-storey buildings are performed under pairs of linearly scaled ground-motions. Both far-field and near-field non-pulselike acceleration series are considered. This study shows that incorporating a spectral shape parameter into the *IM*-vector reductions of up to 40 % can be obtained on conditional standard deviations when assessing bi-directionally loaded 3D buildings. The effects of alternative framing systems on structural fragilities are found to differ depending on the number of storeys. For 6-storey structures, consistently higher capacities are observed in two-way layouts with respect to one-way systems as well as increasing variabilities at larger demand levels. Finally, drift hazard curves are calculated by combining the building fragilities with idealized ground-motion hazard estimates. The results indicate that one-way buildings experience consistently lower drift exceedance rates regardless of the ground-motion type, especially for drift levels larger than 2 % although the differences are larger for the 9-storey frames in comparison with their 6-storey counterparts.

Keywords: steel framing systems, bi-directional seismic loads, 3D steel frames, seismic fragilities, performance-based seismic assessment

1. Introduction

Distinct structural systems prevail in different regions of the world depending on the construction skills, history and industrial context of each particular community. This is the case of Japan on the one hand and North America and Europe on the other where two distinguishable steel framing systems have been traditionally employed. Japanese engineers have usually adopted a two-way layout consisting of 3D beam-column assemblages designed to resist seismic and gravity loads simultaneously [1]. By contrast, American and European seismic codes differentiate clearly between primary and secondary lateral resisting systems and seek to provide the primary frames with adequate seismic strength and ductility while the secondary (or gravity) frames are designed to resist gravity loads only. These secondary frames, which initially do not contribute significantly in terms of base shear or stiffness, are known to exhibit large elastic deformation capacities and can enhance the overall post-elastic response of the building if properly designed [2]. Therefore, the question arises as to which of the two building configurations (one-way or two-way frames) has a better performance at different levels of seismic demand.

Likewise, although the importance of considering bi-directional earthquake actions in structural assessments has long been recognised [3] including the development of simplified assessment and modelling procedures [4], comparative studies on the behaviour of different framing systems under bi-directional loads are lacking and no previous study has taken advantage of the benefits brought about by vector-based approaches. Liao et al. [5] developed 3D models of 3-storey Moment Resisting Frame (MRF) buildings with pre and post-Northridge connection details and used them to evaluate the effects of connection fracture, gravity frame contribution and column deformation on the whole building performance. Although not directly addressing the influence of alternative framing systems, this study indicated that pre-Northridge buildings have a much higher probability of failure than the newer designs at all performance levels. Tagawa et al. [1] evaluated the seismic performance of two 3-storey 3D building models with one-way and two-way frames through inelastic dynamic analyses. It was shown that the two-way framing layout had a smaller mean annual probability of exceedence for inter-storey drifts of less than 3 % whereas larger mean annual probabilities of exceedence were observed for greater drifts. Nevertheless, this study focused only on 3-storey MRFs, used Spectral Acceleration as the single scalar ground-motion intensity measure, and applied single-component recorded acceleration records at 450 to the building axes.

Given the uncertainties involved, the evaluation of the performance of alternative framing systems ought to be carried out within an explicit probabilistic framework, the formalization of which came about one and a half decades ago in the form of guidelines published by the US Federal Emergency Management Agency (FEMA) [6]. Such probabilistic assessment framework can be expressed as:

$$\lambda_{EDP} = \int_{IM} P(EDP > x | IM = im) x |d\lambda_{IM}(im)| \quad (1)$$

where $\lambda_{EDP}(x)$ is the mean annual rate of exceeding a certain value of EDP , EDP stands for Engineering Demand Parameter and represents the variable under which judgements can be made in terms of structural performance, and IM stands for Intensity Measure and defines the ground-motion intensity at the site under study. In the case of steel MRF, the EDP of choice is customarily the maximum inter-storey drift, θ_{max} , due to the strong correlation between θ_{max} and earthquake damage, while the elastic 5 %-damped Spectral Acceleration at the first structural period, $S_a(T_1)$, is usually taken as the intensity measure thus making IM both site as well as structure specific. Besides, the first term of the product inside the integral in Equation 1 is commonly referred to as the fragility of the structure. It expresses the probability of exceeding the EDP value of interest given that the IM admits a certain value, im . Similarly, the second term inside the integral in Eq. (1) is the site hazard (i.e. the mean annual rate of exceeding a value of IM). It should be noted that under this definition, im is a scalar quantity and therefore Eq. (1) presupposes that the ground-motion can be well-characterized by a single parameter.

The possible lack of sufficiency of a single intensity parameter to characterize the ground-motion has lead researchers to express the above mentioned probabilistic assessment framework in vector form [7]. The sufficiency of an IM is associated with the degree to which the conditional probability distribution referred to in Eq. (1) is independent from other ground-motion parameters. It is an intuitive remark that a complicated

phenomenon such as an earthquake ground-motion cannot be described by a single intensity measure, even if this is structure specific in a particular way. With this purpose, Eq. (1) can be reformulated as:

$$\lambda_{EDP} = \int_{IM_1} \int_{IM_2} P(EDP > x | IM_1 = im_1, IM_2 = im_2) x |d\lambda_{IM_1, IM_2}(im_1, im_2)| \quad (2)$$

which involves two Intensity Measures (IM_1 and IM_2). The concept can be extended if more than two intensity measures are considered. By taking into account more ground-motion parameters, improved estimations of structural response are expected which should allow for a better performance assessment. Although vector-valued approaches are considered as a simple extension of the scalar case, their practical implementation has not been well established [8] and the identification of a suitable vector of IM remains constrained by the availability of adequate prediction equations and by the efficiency of their combination [9]. An efficient IM set will allow for a reduced variability in the quantification of the structural response, hence decreasing the standard error on the sample mean of the EDP and potentially cutting down the number of analyses required to achieve a given accuracy in the response estimation. To this end, Faggella *et al.* [10] performed a probabilistic evaluation of the 3D seismic response of a single reinforced-concrete building and identified the shortcomings of using $S_a(T_1)$ as the only IM . The authors advocated strongly for the use of vector formulations when 3D structures are considered. However, they did not perform a vector- IM -based assessment of probabilistic demands. Similarly, no comparative assessment of the response of multi-storey mid-rise buildings with different framing layouts have been carried out to date, especially from a vector-valued seismic assessment perspective.

In light of the above discussion, this study seeks to offer a detailed comparison of the response of alternative framing configurations (i.e. one-way and two-way systems) subjected to bi-directional earthquake loading within a probabilistic assessment framework. Both vector-valued as well as scalar based comparisons are performed. Particular attention is given to the quantification of the benefits of employing a vector-valued assessment over a scalar formulation when evaluating maximum inter-storey drift demands in 3D buildings. Practical aspects related to the bi-directional loading and parameter definition are then introduced and fragility curves as well as fragility surfaces are defined for two-way and one-way structures characterized by means of scalar and vector formulations, respectively. The results presented constitute a first attempt to implement a vector-based comparison of the world's two most prevailing steel framing systems subjected to bi-directional ground-motion and represent an important step towards identifying the steel-framing layout with the most favourable seismic performance at different demand levels.

2. Structural systems and earthquake ground-motions

Fig. 1 presents the layout of the two main framing systems examined in this study, namely: one-way and two-way frames. As noted above, two-way buildings are designed such that all structural elements resist lateral loads. On the other hand, a few selected frames (usually towards the building perimeter) are designed to sustain the entirety of lateral actions in one-way buildings, while the other frames are assumed to carry gravity loads only. Symmetric five bay-by-five bay layouts with 5.00 m width per bay and 5 % mass-eccentricity are examined. It is believed that these can offer an insight into the general behavioural trends of the two building systems analysed and provide a good basis for future studies incorporating a wider range of geometric variations. Besides, the symmetric nature of the frames under study facilitates the analysis of the extent to which different vectors of IM influence the response estimation. The storey height is kept constant at 3 m while 6-storey and 9-storey buildings are considered making a total of 4 building models. W14x38 and W12x35 beams were employed for the lower 4 and upper 2 storeys in 6-storey buildings, respectively. Similarly, W14x38 to W14x30 sections were used for the 9-storey building. Square hollow sections ranging between 400x400x16 mm and 300x300x12.5 mm were employed for the columns in two-way frames while HEB400 to HEB320 column sections were used in one-way buildings. More specific details of the frames can be found elsewhere [11].

The onerous computational demands associated with bi-directional response-history analyses are alleviated herein by employing equivalent fish-bone models of reduced number of degrees of freedom to represent the buildings as schematically depicted in Fig. 2. In the case of one-way structures (Fig. 2b), the lateral resisting frames acting primarily in-plane are simulated by four primary frames with pin-ended beams fully fixed to the columns. In turn, all the gravity frames are summed up in a single continuous column connected to the

other frames by means of rigid diaphragm constraints. On the other hand, the two-way framed buildings (Fig. 2a) are modelled with four columns and fully fixed beam-to-column connections at both beam ends. The adequacy of these simplified models to estimate peak deformations of multi-storey buildings, including bi-directionally loaded ones, has been extensively established in previous studies [12, 13]. To this end, fibre-based FE models were constructed in OpenSees [14] by means of force-based elements accounting for material and geometric non-linearities. A superimposed load of 3000 N/m² was used in all storeys. A Bilinear steel material model was considered with an Elastic Modulus of 210 GPa and 3 % post-elastic strain hardening. The FE models employed and their fundamental modes are depicted in Fig. 3.

The two sets of acceleration series suggested by the Federal Emergency Management Agency [15] were employed herein including far-field and near-field non-pulselike records. All 14 pairs of records in the near-field category with no pulses as proposed in [15] were considered as well as the first 16 record pairs with the largest geometric mean peak ground accelerations (PGA_{GM}) form the far-field set. The original un-scaled series available in the NGA-West2 database [16] were employed. Since this work is concerned with bi-directional analyses, the axis orientation of the horizontal acceleration components was randomized following the findings of Beyer and Bommer [17] who noted that the response to horizontal ground-motion components with randomly oriented axes can be used for the estimation of unbiased median EDP responses. This was particularly relevant for the near-field pairs, which were consistently reported in the fault-parallel and fault-normal directions in their original form [15, 16]. Further details of the records employed can be found in [18]

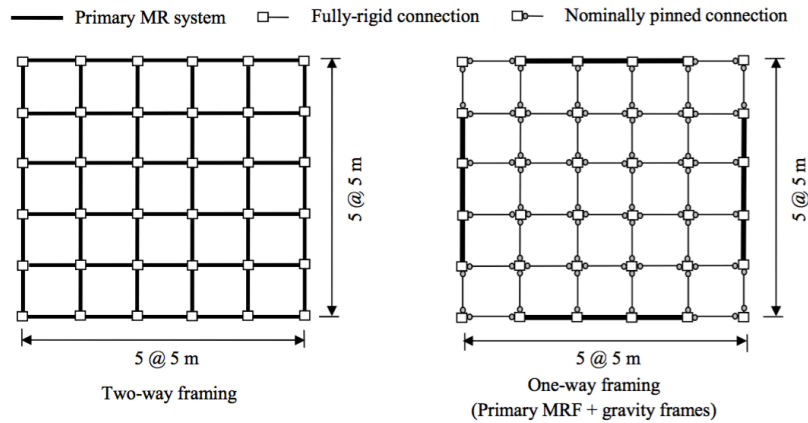


Fig. 1 – Framing systems layout

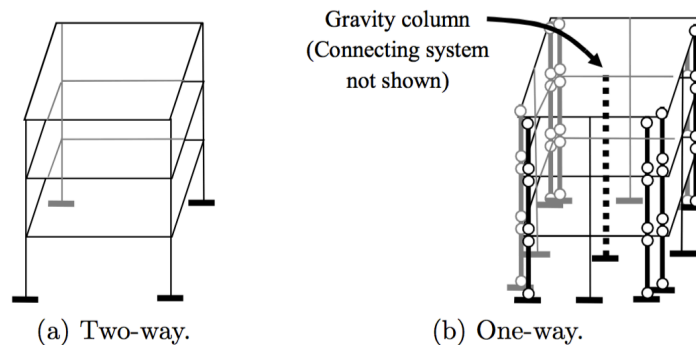


Fig. 2 – Simplified 3D fish-bone models employed

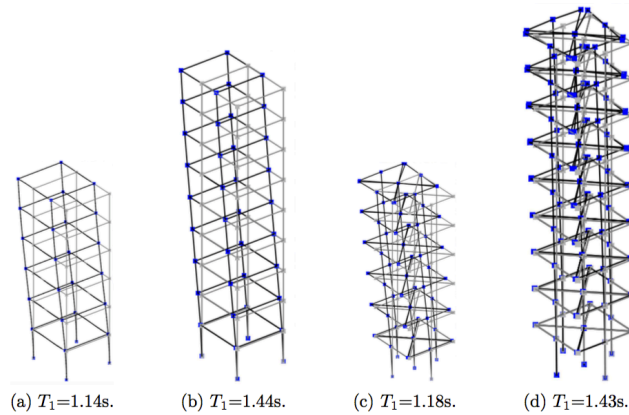


Fig. 3 – Fundamental vibration modes: (a) 6-storey two-way, (b) 9-storey two-way, (c) 6-storey one-way, and (d) 9-storey one-way

3. Nonlinear response history analysis and IMs

A series of non-linear response history analyses were performed on the FE models described above by linearly scaling each pair of ground-motion records to pre-defined levels of intensity. The hunt and fill algorithm proposed by Vamvatsikos and Cornell [19] was applied to this effect while spline interpolation was used to join the discrete points and to obtain continuous *IM* versus *EDP* relationships. Since this paper is concerned with the bi-directional response of 3D models, ground-motion scaling was performed on the spectral acceleration of the geometric mean of the two horizontal components, $S_{a,GM}$. This is particularly relevant to the structures considered here since they are symmetric (i.e. $T_1 \approx T_2$). Similarly, the absolute maximum inter-storey drift along the height of the building, θ_{max} , was taken as the EDP. Also, since the interest of this study is on the slight to extensive damage states that tend to dominate loss estimates rather than on collapse prediction, a target maximum drift of $\theta_{max} = 7\%$ was employed to set the limits of analysis. As noted by [20], care should be taken when utilizing linearly scaled ground-motion records within a vector-*IM* based framework. This is due to the fact that different intensity measures scale differently for the same scaling level. However, ground-motion scaling was considered adequate for the present study since its main interest lies in the identification of behavioural trends for which the preservation of the natural correlations between *IMs* is not of primary importance. Furthermore, none of the secondary *IM* employed scales with spectral ordinates and therefore consistency is maintained among all studied combinations of parameters.

From a structural engineer's perspective, the selection of a second intensity measure, IM_2 in Eq. (2), should be such that the requirements for more demanding calculations are balanced by an improvement in the explanation of the structural response. To this end, besides the spectral acceleration $S_{a,GM}(T_1)$, four additional ground-motion parameters were employed to construct vectors of *IM*, including:

- the spectral acceleration ratio, R_{T_3, T_1} , which is the ratio between the spectral accelerations at the third and first structural periods, $S_{a,GM}(T_3)$ and $S_{a,GM}(T_1)$, respectively. Given the symmetric nature of the buildings analysed where $T_1 \approx T_2$, the third period was selected in order to consider the effects of higher modes in the structural response while keeping the estimate of R_{T_3, T_1} stable.
- the spectral shape parameter, N_p . This parameter was proposed by Bojorquez and Iervolino [21] and was defined as the average of unidirectional spectral ordinates normalized by $S_a(T_1)$. The efficiency of the vector $\langle IM_1, IM_2 \rangle = \langle S_a, N_p \rangle$ has been proved for planar structures [21]. In the present study, this parameter is extended to bi-directional ground-motion by operating over the geometric mean of the two horizontal components such that:

$$N_p = \frac{S_{a,avg}(T_1 \dots T_N)}{S_{a,GM}(T_1)} = \frac{(\prod_{i=1}^N S_{a,GM}(T_i))^{1/N}}{S_{a,GM}(T_1)} \quad (3)$$

where T_N is a period that defines the portion of the spectrum to the right of the elastic period that is considered for the characterization of the ground-motion. It follows that N_p aims to incorporate the

effects of inelastic periods in the ground-motion characterization. A value of $T_N = 2T_l$ and a step of $\Delta T_i = 0.001$ second was used herein which enabled stable estimates of N_p to be made. Although ground-motion models do not currently exist to predict N_p , they can be obtained on the basis of a prediction equation for spectral accelerations and a correlation model for different spectral ordinates as will be shown.

- finally the frequency content parameters, T_m and T_o , were also included in the seismic assessment. Importantly, ground-motion prediction equations have already been developed for the estimation of T_m and T_o [22]. Besides, the Mean Period, T_m of the ground-motion has been previously found to improve the estimation of peak displacements in steel structures [23,24] subjected to one-directional loading. T_m is calculated by weighting the amplitudes of the Fourier Spectrum as follows:

$$T_m = \frac{\sum_i \beta_i^2 \frac{1}{f_i}}{\sum_i \beta_i^2} \quad \text{for } 0.25 \text{ Hz} \leq f_i \leq 20 \text{ Hz} \quad (4)$$

where β_i is the Fourier Amplitude Coefficient at frequency f_i . A minimum frequency step of $\Delta f \leq 0.05$ Hz is used for the Fourier Transform in order to get a stable representation of its frequency content [22]

Additionally, the Smoothed Predominant Period, T_o , which is based on the 5 %-damped elastic response spectrum rather than the Fourier spectrum was also evaluated. T_o is defined as:

$$T_o = \frac{\sum_i T_i \ln\left(\frac{S_a(T_i)}{PGA}\right)}{\sum_i \ln\left(\frac{S_a(T_i)}{PGA}\right)} \quad \text{for } T_i \text{ with } \frac{S_a(T_i)}{PGA} \geq 1.2 \quad (5)$$

Therefore, only the periods for which $S_a \geq 1.2 PGA$ are considered in the calculation of T_o while equal spacing is adopted in the logarithmic space. As a result, T_o is more representative of the high to moderate frequencies in the spectrum.

It is important to note that the calculation of all ground-motion parameters have to be carried out in consistency with the bi-directional nature of the analyses carried out in this study. To this end, the Fourier amplitude coefficients in Eq. (4) were combined by means of the Euclidean norm when calculating T_m while a Geometric Mean spectrum was used for the computation of T_o , N_p and $R_{T3,T1}$.

Extensive analyses were performed by subjecting the 3D FE models described above to the two sets of ground-motion pairs previously introduced. Linear ground-motion scaling was applied as outlined in the previous section and the corresponding peak deformations were recorded. The data gathered forms the basis for the statistical analyses that follow. The estimation of fragility capacity relationships for the four models under study at different damage states and considering both scalar as well as vector intensity measures as well as one-way and two-way frames is presented below.

4. Fragility estimations

This section deals with the first multiplication terms inside the integrals of Eqs. (1) and (2). that express the probability of exceeding a given value of EDP conditional on the intensity of the ground-motion. This function corresponds to a fragility curve if a scalar IM is employed and to a fragility surface if a IM -vector is used.

When the distribution of the EDP is assumed to be conditional on a single ground-motion characteristic, a scalar IM can be considered and the complementary cumulative distribution function, which defines the probability $P(EDP > x | IM = im)$, can be estimated directly. A log-normal distribution of IM conditional on a given level of EDP can be fitted to the numerical data [25]. The cumulative distribution function, $P(EDP > x | IM = im)$, is then used as the fragility function. The method of moments was applied herein in order to estimate the log-normal distribution parameters [26] such that:

$$\mu_{\ln IM} = \frac{1}{N} \sum_{i=1}^N \ln IM_i \quad (6)$$

$$\sigma_{\ln IM} = \sqrt{\frac{1}{N-1} \sum_{i=1}^N (\ln IM_i - \mu_{\ln IM})^2} \quad (7)$$

This procedure is illustrated in Fig. 4 for a limit state defined by $\theta_{max} = 0.05$ and for the four structures examined in this study when subjected to far field records.

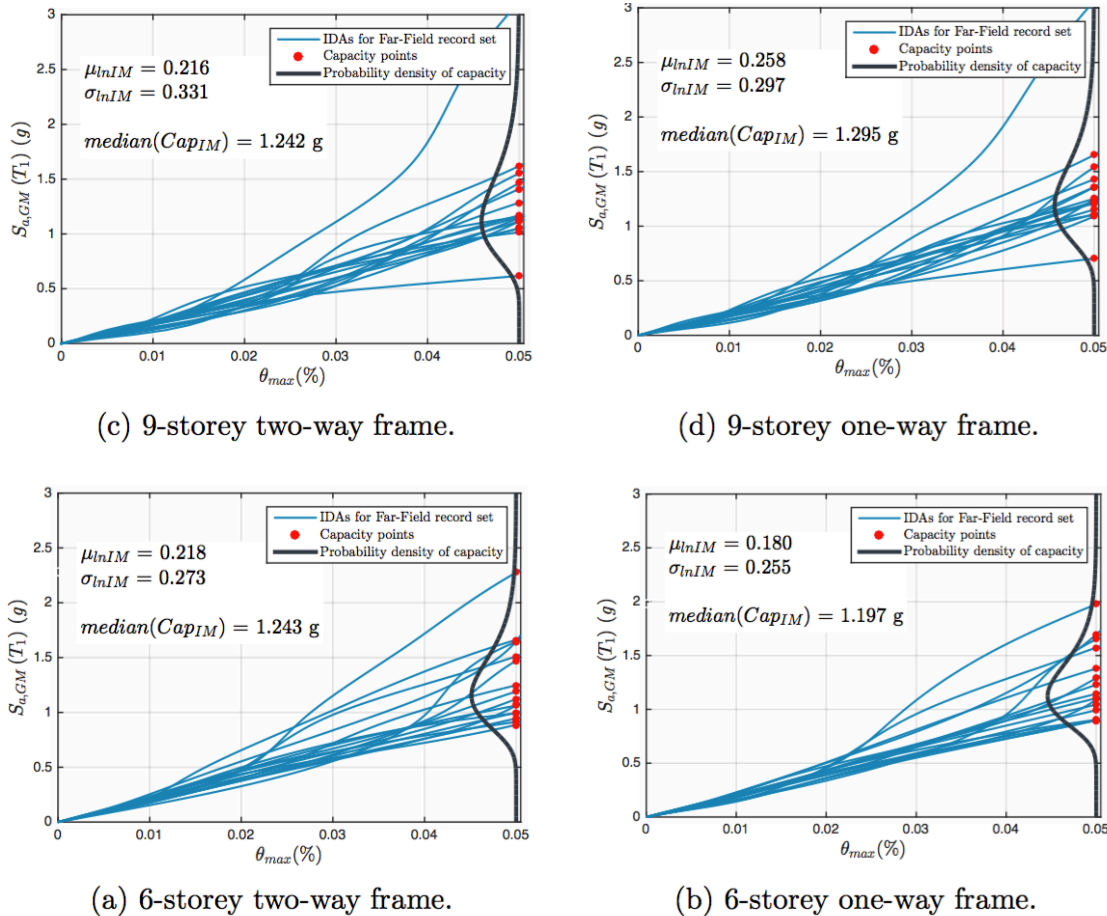


Fig. 4 – Scalar fragilities for 5 % peak drift limit. Far-field records.

In total, three different statistical modelling approaches were evaluated in terms of their applicability to the estimation of fragility surfaces of bi-directionally excited 3D buildings. These included Logistic Regression initially proposed by Shome and Cornell [27], the improved logistic regression methodology proposed by Bojorquez *et al.* [28] as well as linear regression [25]. A more detailed discussion on the issues encountered while implementing these methods can be found elsewhere [18].

Fig. 5 presents a fragility surface obtained by means of linear regression for the 6-storey two-way frame considering N_p as secondary intensity measure while Fig. 6 presents similar results for $R_{T3,T1}$ and $S_{a,GM}(T_3)$. The corresponding linear regression fitting is also shown in Fig. 6. The coefficient of determination is included as a goodness of fit measure. Additionally, the p-value of the b_1 coefficient defined as the T-statistic of the null hypothesis for the statistical significance of b_1 (i.e. $b_1=0$) is also reported. A small value of p implies the statistical significance of the second IM. It should be noted that problems may arise when implementing linear regression with vectors incorporating strongly correlated IMs. The case of $S_{a,GM}(T_3)$ is presented in Figures 8c and 8d as an example. It can be seen from these figures that the positive correlation between IM1 and IM2 has led to very high values of $P(EDP > x)$ at low $S_{a,GM}(T_1)$ levels which can be unsuitable for coupling fragilities and hazard estimations. Similar problems have been reported in [8] when a linear combination of $S_a(T_1)$ and $S_a(T_2)$ was used as a scalar IM. On the other hand, the dimensionless ratio $R_{T3,T1}$ computed from the geometric mean spectrum is shown to produce better results in Figure 6a.

The results indicated that by and large, very little further explanation of the structural response is provided by T_o since the fragility surfaces were conditional almost exclusively on $S_{a,GM}(T_1)$ when $\{S_{a,GM}, T_o\}$ was used. On the other hand, including the mean period, T_m (calculated from the Euclidean norm of the Fourier spectra of the two ground-motion components) in the IM vector leads to a moderate improvement of the fragility estimations at lower drifts for the 9-storey building and under far-field ground-motions only. In this case, the p-values at the $\theta_{max} = 0.007$ limit are 0.106 and 0.136 for two-way and one-way frames, respectively while a reduction of around 5 % in the dispersion is brought about by including T_m in the vector of IM s. Also, a minor tendency of T_m to be more efficient for the 9-storey two-way frame than for the 9-storey one-way structure was observed. Besides, the mild benefits described above for the vector $\{S_{a,GM}, T_m\}$ are absent when near-field earthquakes are employed.

The spectral ratio, R_{T_3, T_1} , as obtained from the geometric mean spectrum was found useful at lower drift limits ($\theta_{max} = 0.007$) for all the structures considered under far-field records. p-values smaller than 0.05 were found in all cases except for the 6-storey one-way building for which a p-value of 0.16 was observed. Even then, this p-value is the smallest of all secondary IM s examined at this level of deformation (i.e. $\theta_{max} = 0.007$). The ability of R_{T_3, T_1} to provide additional explanation of the structural response diminishes with increasing drift values. This is a direct consequence of the higher mode dependence of the response at small θ_{max} values which period range is well characterized by R_{T_3, T_1} . As the deformation increases, plastic behaviour introduces increasing levels of period lengthening, hence altering the range of periods governing the structural response.

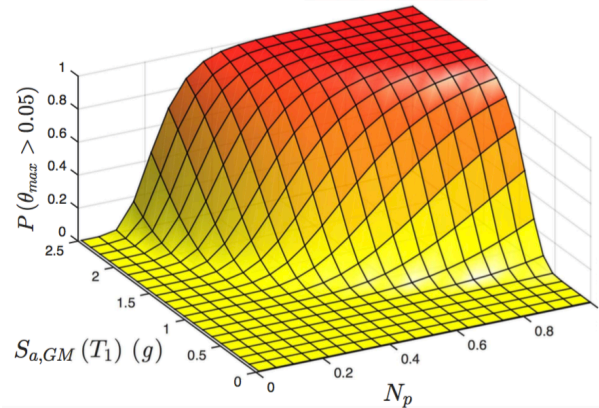


Fig. 5 – Linear regression for $\{S_{a,GM}, N_p\}$ for the $\theta_{max} = 0.05$ limit, 6-storey two-way frame

A more favourable performance was observed for the spectral shape parameter, N_p , obtained from the geometric mean spectrum, at larger deformations. All fragility estimations at large peak drifts (i.e. $\theta_{max} = 0.05$) were affected significantly by the consideration of N_p as a secondary IM . This is true regardless of the framing system under consideration and hold for both far-field and near-field ground-motion sets, although lower improvements were evident for near-field relative to far-field records. On the other hand, the statistical significance of N_p was rather small for lower levels of peak drift. Very small p-values are obtained in all $\theta_{max} = 0.05$ cases with reductions in the corresponding standard deviation of up to 40 % in the case of 9-storey buildings (both one-way and two-way) subjected to far-field acceleration series when compared with the scalar case. However, smaller reductions of standard deviation, in the order of 20 %, were observed for 6-storey structures. In the case of near-field actions these reductions are 30 % and 10 % for 9 and 6-storey buildings, respectively. Additionally, it should be noted that around 40 % and 66 % of the variance of the scalar IM can be explained by the secondary IM in $\{S_{a,GM}, N_p\}$ in the case of 6- and 9-storey structures, respectively. These values are reduced to 20 % and 50 % for the 6- and 9-storey buildings when near-field ground-motion pairs are considered. The stronger performance of N_p for 9-storey buildings indicates that the variability in the response of these structures is associated with their non-linear response to a greater degree than for 6-storey structures.

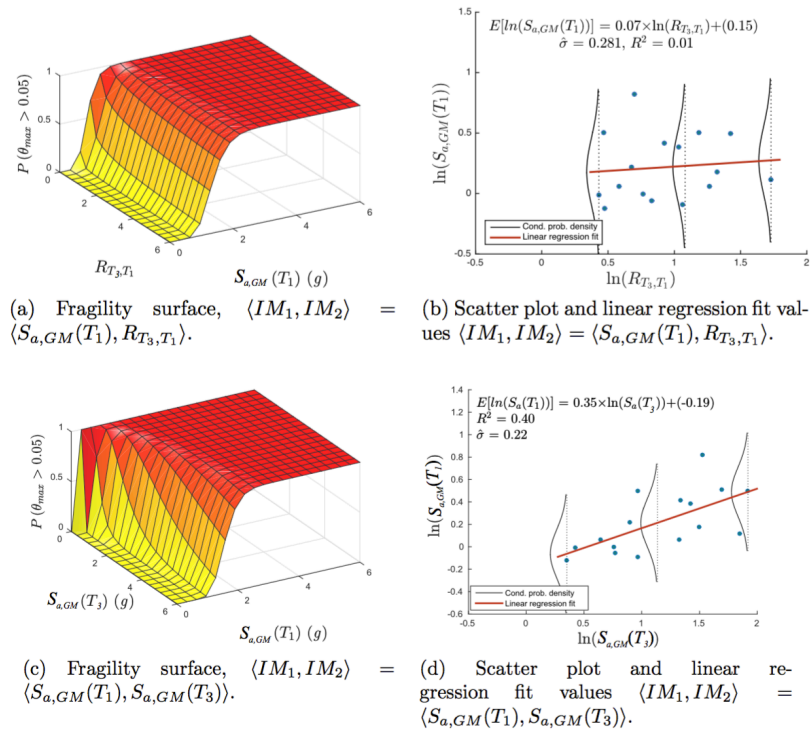


Fig. 6 – Scalar fragilities for 5 % peak drift limit. Far-field records.

5. Simplified drift hazard estimations

Simplified seismic scenarios associated with punctual sources located at 16 and 4 km from the building site in consistency with the far-field and near-field assumptions, respectively, are utilized. It is fully recognized that simplifying the seismic hazard to a point source is not necessarily comparable with a real Probabilistic Seismic Hazard Assessment for which several sources are usually considered. Despite these simplifying assumptions, important general tendencies can be identified as will be discussed in the following sections. Finally, only the results for the scalar $IM_1 = S_{a,GM}$ and the vector $\langle IM_1, IM_2 \rangle = \langle S_{a,GM}, N_p \rangle$ cases are presented for brevity. In light of the single distance assumption, the Marginal Moment Distribution can be taken as the joint distribution of magnitude and distance. To this end, a doubly-bounded Gutenberg-Richter exponential distribution with $b = 1.0$ was assumed and 5 and 7 minimum and maximum Moment values, respectively. The Boore and Atkinson [29] ground-motion prediction model was used herein in light of its simplicity.

The second term in Eq. (1) and (2) is known as the mean rate density (*MRD*). In the case of a vector-IM formulation, the MRD is defined as:

$$MRD_{IM_1, IM_2}(im_1, im_2) = \sum_{i=1}^N v_i \left(\int_R \int_M f_{IM_1, IM_2}(im_1, im_2 | m, r) f_{M,R}(m, r) dm dr \right)_i \quad (8)$$

This equation now requires the specification of a joint distribution of IMs given an earthquake scenario of the form $f_{IM_1, IM_2}(im_1, im_2 | m, r)$. This distribution can be decomposed into the product of a marginal distribution of IM_1 , as defined in Eq. (2), and a conditional distribution of IM_2 conditional on IM_1 . Assuming log-normality, this conditional distribution can be represented by:

$$\mu_{\ln IM_2 | im_1, m, r} = \mu_{\ln IM_2 | m, r} + \rho_{IM_1, IM_2} \frac{\sigma_{\ln IM_2 | m, r}}{\sigma_{\ln IM_1 | m, r}} (\ln im_1 - \mu_{\ln IM_1 | m, r}) \quad (9)$$

$$\sigma_{\ln IM_2 | im_1, m, r} = \sigma_{\ln IM_2 | m, r} \sqrt{1 - \rho_{IM_1, IM_2}^2} \quad (10)$$

where $\mu_{\ln IM_2 | m, r}$ and $\sigma_{\ln IM_2 | m, r}$ are the logarithmic mean and standard deviation of the marginal distribution of IM_2 , respectively and ρ_{IM_1, IM_2} is the correlation between the two *IMs*. If N_p is considered as secondary intensity

measure, these parameters can be obtained starting from Eq. (3) [18]. In the original study [21], N_p was employed within a seismic hazard assessment framework based on a log-normally distributed hybrid scalar intensity measure IN_p instead of performing a full vector-valued probabilistic seismic hazard analysis. IN_p was defined in [21] as a linear combination of the logarithm of N_p and $S_a(T_1)$. However, the use of such intensity measure would require the site seismic hazard to be dependent on the fragility of the structure as explained in [18]. In the present study, in order to allow for a site seismic hazard for the vector-IM, a direct correlation function between $\ln S_a(T_1)$ and $\ln N_p$ was sought such that:

$$COV[\ln N_p, S_{a,GM}(T_1)] = COV[\ln S_{a,GM,avg}(T_1 \dots T_N), \ln S_{a,GM}(T_1)] - COV[\ln S_{a,GM}(T_1), S_{a,GM}(T_1)] \quad (11)$$

$$\rho_{\ln N_p, [S_{a,GM}(T_1)]} = \frac{\rho_{\ln [S_{a,GM,avg}(T_1 \dots T_N)], \ln [S_{a,GM}(T_1)]} \sigma_{\ln [S_{a,GM,avg}(T_1 \dots T_N)]} \sigma_{\ln [S_{a,GM}(T_1)]} - \sigma_{\ln [S_{a,GM}(T_1)]}^2 \sigma_{\ln [S_{a,GM}(T_1)]}}{\sigma_{\ln N_p} \sigma_{\ln [S_{a,GM}(T_1)]}} \quad (12)$$

6. Response comparison of alternative framing systems

Fig. 7 presents a typical comparison of the drift hazard curves obtained by means of the scalar, $IM = S_{a,GM}(T_1)$, and vector, $\{IM_1, IM_2\} = \{S_{a,GM}(T_1), N_p\}$ models outlined above for the far-field record set. It is evident from this figure that by considering the shape factor parameter, N_p , as a secondary IM a higher proportion of the structural response is explained leading to lower drift exceedance rates, especially at larger peak drift levels ($\theta_{max} > 0.02$). For example, the consideration of the vector $\{S_{a,GM}(T_1), N_p\}$ reduces the hazard in about 50% for $\theta_{max} = 0.05$. The effects of a reduced dispersion brought about by the secondary IM were larger for far-field than for near-field records.

A direct comparison of the effects of alternative framing configurations, including the positive reductions in the dispersion $\sigma_{\ln IM}$ introduced by the vector approach, can be established with reference to the drift hazard curves depicted in Fig. 8. To this end, Figs. 8a and 8b present a comparative assessment of structures with one-way and two-way framing systems under far-field and non-pulselike near-field ground-motions, respectively. These curves have been obtained following the procedure outlined in the previous section. It can be appreciated from these figures that the responses of 6- and 9-storey structures follow clear and differentiated trends with higher hazards associated with 6-storey buildings regardless of the ground-motion type. Also, it is evident from Fig. 8 that one-way buildings experience consistently lower drift exceedance rates, especially for drift levels larger than 2%. The smaller drift hazards experienced by one-way systems relative to two-way frames are more evident for 9-storey structures and become more significant as the drift demand level increases. The lower variability and slightly higher relative capacities associated with one-way frames at larger drifts together with the presence of gravity frames that are able to mitigate the second-order effects and can reduce the concentration of plastic deformations explain this behaviour.

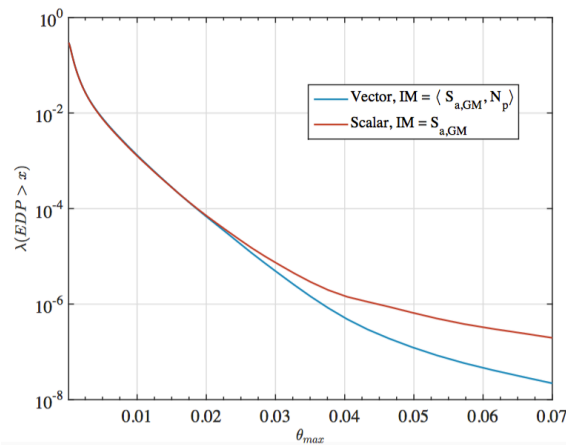


Fig. 7 – Comparison of drift hazard curves obtained with scalar and vector IM. 9-storey two-way frame.

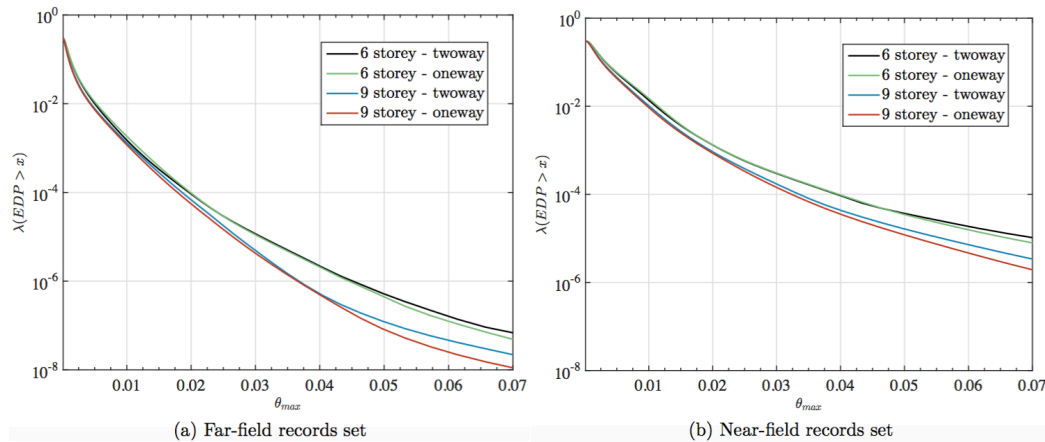


Fig. 8 – Comparison of drift hazard curves obtained with scalar and vector IM. 9-storey two-way frame. Far-field records.

7. Conclusions

The following findings can be offered in relation to the relative seismic performance of one-way and two-way building layouts:

- One-way framing systems experience consistently lower drift exceedance rates than two-way frames for drift demands of $\theta_{max} > 0.02$. This differences between the drift hazards of one-way and two-way buildings are more evident for 9-storey structures and become more significant as the deformation demands increase. These trends are attributed to the lower variability on the response of one-way buildings coupled with the presence of gravity frames that help to mitigate second-order effects and reduce the concentration of plastic deformations.
- When simplified (single-point source) seismic hazard is assumed, higher drift hazards are experienced by 6-storey buildings in comparison with their 9-storey counterparts regardless of the ground-motion type or framing system adopted.
- Different tendencies are observed for the fragilities of two-way and one-way framing systems depending on the number of storeys. In the case of 6-storey structures, consistently higher capacities are observed for two-way layouts at all peak drift limits for both near-field and far-field records. Conversely, 5 % lower mean capacities are obtained for two-way frames in 9-storey buildings. These differences can be attributed to the increased effect of second order actions in taller structures coupled with the susceptibility of two-way frames to the simultaneous formation of plastic hinges in all its lateral resisting elements. In contrast, the gravity frames present in one-way configurations do not experience plastic demands up to large drifts thus making one-way configurations inherently more resilient to the effects of second-order forces which will be higher in 9-storey than in 6-storey structures. The stronger performance of the ground-motion shape parameter, N_p , for 9-storey buildings also points towards a greater influence of plastic deformation patters in the response of these structures.
- Also, it was observed that around 40 % and 66 % of the variance of the scalar IM can be explained by the secondary IM in $\{S_{a,GM}, N_p\}$ in the case of 6- and 9-storey 3D structures, respectively, subjected to far-field acceleration pairs. These values are reduced to 20 % and 50 % for the 6- and 9-storey buildings when near-field ground-motion pairs are considered.
- At lower drift levels (e.g. $\theta_{max} = 0.007$), the spectral ratio, $R_{T3,T1}$, produces statistically significant enhancements in the estimation of the response for all the structures considered under far-field records. The associated reductions in standard deviation are in the order of 10 % with respect to scalar formulations. Similarly, approximately 25 % of the variance of the scalar IM can be explained by $R_{T3,T1}$ acting as secondary IM . In contrast, when near-field responses are considered, the inclusion of $R_{T3,T1}$ as secondary IM seems to bring limited benefits for all 3D building configurations examined.

9. References

- [1] Tagawa H, MacRae G, Lowes L (2008): Probabilistic evaluation of seismic performance of 3-story 3D one- and two-way steel moment-frame structures. *Earthquake Engineering and Structural Dynamics*, 37, 681-696.
- [2] Málaga-Chuquitaype C, Elghazouli AY, Enache R (2016): Contribution of secondary frames to the mitigation of collapse in steel buildings subjected to extreme loads. *Structure and Infrastructure Engineering*, 12(1), 45-60.
- [3] Chopra AK, Goel RK (1991): Evaluation of torsional provisions in seismic codes. *Journal of Structural Engineering, American Society of Civil Engineers*, 117, 3783-3803.
- [4] Chopra AK, Goel RK (2004): A modal pushover analysis procedure to estimate seismic demands for unsymmetric plan buildings. *Earthquake Engineering and Structural Dynamics*, 33, 903-927.
- [5] Liao KW, Wen YK, Foutch DA (2007): Evaluation of 3d steel moment frames under earthquake excitations: 1: Modeling. *Journal of Structural Engineering, American Society of Civil Engineers*, 133, 462-470.
- [6] Cornell CA, Jalayer F, Hamburger RO, Foutch DA (2002): Probabilistic Basis for 2000 SAC Federal Emergency Management Agency Steel Moment Frame Guidelines. *Journal of Structural Engineering*, 128, 526-533.
- [7] Bazzurro P (1998): *Probabilistic seismic demand analysis*. Ph.D. Dissertation, Stanford University, CA, US.
- [8] Gehl P, Seyedi D, Douglas J (2013): Vector-valued fragility functions for seismic risk evaluation. *Bulletin of Earthquake Engineering*, 11, 365-384.
- [9] Luco N, Cornell CA (2007): Structure-specific scalar intensity measures for near-source and ordinary earthquake ground motions. *Earthquake Spectra*, 23, 357-392.
- [10] Faggella M, Barbosa AR, Conte JP, Spacone E, Restrepo JI (2013): Probabilistic seismic response analysis of a 3-D reinforced concrete building. *Structural Safety*, 44, 11-27.
- [11] Málaga-Chuquitaype C (2011): *Seismic design and assessment of steel structures incorporating tubular members*. Ph.D. Thesis, Imperial College London, UK.
- [12] Nakashima M, Ogawa K, Inoue K (2002): Generic frame model for simulation of earthquake responses of steel moment frames. *Earthquake Engineering and Structural Dynamics*, 31, 671-692.
- [13] Luco N, Mori Y, Funahashi Y, Cornell A, Nakashima M (2003): Evaluation of predictors of non-linear seismic demands using fishbone models of SMRF buildings. *Earthquake Engineering and Structural Dynamics*, 2267-2288.
- [14] McKenna F, Fenves GL, Scott M (2000): *Open System for Earthquake Engineering Simulation*, Pacific Earthquake Engineering Research Center, University of California at Berkeley, CA, US.
- [15] Federal Emergency Management Administration (2009): *Quantification of building seismic performance factors*, Technical Report, FEMA P695
- [16] Ancheta TD, Darragh RB, Stewart JP, Seyhan E, Silva WJ, Chiou B, Wooddell KE, Graves RW, Kottke AR, Boore DM (2014): NGA-West2 database. *Earthquake Spectra*, 30, 989-1005.
- [17] Beyer K, Bommer JJ (2007): Selection and Scaling of Real Accelerograms for Bi-Directional Loading: A Review of Current Practice and Code Provisions. *Journal of Earthquake Engineering*, 11, 13-45.
- [18] Málaga-Chuquitaype C, Bougatsas, K (2017): Vector-IM-based assessment of alternative framing systems under bi-directional ground-motion. Submitted
- [19] Vamvatsikos D, Cornell CA (2002): Incremental dynamic analysis. *Earthquake Engineering and Structural Dynamics*, 31, 491-514.
- [20] Modica A, Stafford PJ (2014): Vector fragility surfaces for reinforced concrete frames in Europe. *Bulletin of Earthquake Engineering*, 12, 1725-1753.
- [21] Bojorquez E, Iervolino, I (2011): Spectral shape proxies and nonlinear structural response. *Soil Dynamics and Earthquake Engineering*, 31, 996-1008.
- [22] Rathje EM, Faraj F, Russell S, Bray JD (2004): Empirical Relationships for Frequency Content Parameters of Earthquake Ground Motions. *Earthquake Spectra*, 20, 119-144.

- [23] Málaga-Chuquitaype C, Elghazouli AY (2012): Inelastic displacement demands in steel structures and their relationship with earthquake frequency content parameters. *Earthquake Engineering and Structural Dynamics*, 41, 831-852.
- [24] Málaga-Chuquitaype C. (2015): Estimation of peak displacements in steel structures through dimensional analysis and the efficiency of alternative ground-motion time and length scales. *Engineering Structures*, 101, 264- 278.
- [25] Baker JW (2007): Probabilistic structural response assessment using vector-valued intensity measures. *Earthquake Engineering and Structural Dynamics*, 36, 1861-1883.
- [26] Baker JW (2015): Efficient Analytical Fragility Function Fitting Using Dynamic Structural Analysis. *Earthquake Spectra*, 31, 579-599.
- [27] Shome N, Cornell CA (2000): Structural Seismic Demand Analysis: Consideration of Collapse, in *Proceedings 8th ACSE Specialty Conference on Probabilistic Mechanics and Structural Reliability*, 1-7.
- [28] Bojorquez E, Iervolino, I, Reyes-Salazar A, Ruiz SE (2012): Comparing vector-valued intensity measures for fragility analysis of steel frames in the case of narrow-band ground motions. *Engineering Structures*, 45, 472-480.
- [29] Boore DM, Atkinson GM (2008): Ground-motion prediction equations for the average horizontal component of PGA, PGV, and 5 %-damped PSA at spectral periods between 0.01 s and 10.0 s. *Earthquake Spectra*, 24, 99-138.